MECHANICAL PROPERTIES OF TiB_2-AlFe COMPOSITE FABRICATED BY THE SPARC PLASMA SINTERING

M. Yoshida and H. Shiraishi

National Institute of Technology, Ube-College
2-14-1 Tokiwadai, Ube, Yamaguchi 755-8555, Japan
yoshida@ube-k.ac.jp

Keywords: Fracture toughness, Vickers hardness, Bending strength, TiB_2

ABSTRACT

We have fabricated TiB_2-AlFe composite by the reaction sintering of elemental powders of Ti , B, Al and Fe using spark plasma sintering. We have succeeded to obtain dense TiB_2-AlFe specimen up to 88vol% of TiB_2 by the sintering at 1373k. It is shown that TiB_2 particles are dispersed uniformly in the AlFe matrix. The size of TiB_2 particles is around 0.2 μm when sintered at 1373K, which increases to 0.5 μm at 1473K. The Vickers hardness as high as 2320Hv and bending strength of 850MPa has been obtained for TiB_2-AlFe with 88vol%TiB_2. The fracture toughness estimated from the indentation crack is 13MPa・$m^{1/2}$. It has been shown that TiB_2–AlFe composite has high hardness, high strength and excellent fracture toughness.

1 INTRODUCTION

Titanium diboride (TiB_2) has many desirable properties such as high hardness (Hv=3400), high melting point (3000K), low density (4500kg/m^3), high electrical resistivity and good corrosion resistance [1]. It is a promising candidate for cutting tools, wear proof parts, aircraft propulsion systems, space vehicle thermal protection and so on. However, a high sintering temperature above 2000K is required to obtain dense TiB_2, and the strength of monolithic TiB_2 sintered at such high temperature is not sufficient [2].

In order to obtain dense and high strength TiB_2 by the sintering at lower temperatures, sintering of TiB_2 with various sintering aid has been investigated [3-8]. Li et al has shown that TiB_2-AlFe composite materials can be fabricated by the combustion synthesis from elemental powders of Ti, B, Fe and Al [6]. They have obtained the Vickers hardness of around 2000 Hv and the bending strength of 600MPa for the TiB_2-AlFe composite with 80vol%TiB_2. They have also shown that the size of TiB_2 particles and the porosity increases as the composition of TiB_2 increases due to rapid heat increase caused by the large formation enthalpy of TiB_2.

In the combustion synthesis method, precise control of the specimen temperature is impossible. High reaction enthalpy of Ti and B causes the rapid heating of the specimens and the grain growth of TiB_2, which bring about deterioration of the mechanical properties. On the other hand, in the spark plasma sintering, specimens are heated directly by applying large electric current to powders. In the spark plasma sintering systems, powders are inserted in a carbon container and pressed with high pressure by massive electrode to achieve high electric conductance, which causes excellent thermal conductance also. Then, a precise control of the specimen temperature is possible in the spark plasma sintering even for the specimen which generates large reaction heat associated with the chemical reaction.

In the present study we have fabricated dense TiB_2 materials by the reaction sintering of Ti and B using spark plasma sintering method with AlFe as sintering aid. We have succeeded to obtain dense and fine grained TiB_2 composite materials with the concentration of TiB_2 as high as 88vol%. The bending strength, Vickers hardness and indentation toughness of TiB_2-AlFe composites have been investigated.

.

2 EXPERIMENTAL METHOD

TiB_2-AlFe composites were fabricated using Al, Fe, Ti and B powders by the reaction sintering using plasma sintering method. The raw materials were commercially available Ti powders (99.9% purity and 10μm diameter), Al powders (99.9% and 10μm), Fe powders (99.9% and 10μm) and B powders (99% and 10μm). The powders were mixed so that 85wt% (88vol%) or 90wt% (92vol%) TiB_2 composite is formed. A graphite die, having an internal diameter of 20mm and a wall thickness of 10mm was filled with $5x10^{-3}$kg of the mixed powders and sealed by two graphite punches and mounted on the equipment, LABOX 625 fabricated by Sinterland Ltd. The mixed powders were heated to the settled temperature between 1373K and 1573K with the rate of 50K/min, kept for 20 minutes, and then furnace cooled to room temperature. The temperature was measured using the infrared radiation thermometer IR-AHS0 fabricated by Chino Corporation. Sintering was performed in a vacuum with a residual pressure of 10Pa. A uniaxial pressure of 20MPa was applied during the sintering.

Scanning electron microscope(SEM) observation was performed using a Hitachi S-4300Y instrument. Before the SEM observation, surfaces of the specimens were polished to #1500 by using diamond abrasive plate and etched by nitric acid. X-ray diffraction patterns were measured using a Rigaku Ultima IV X-ray diffractometer with Cu-kα radiation source. Vickers hardness was measured using an Akashi AVK-A hardness tester with the load up to 490N and pressing time of 15 seconds. To perform the bending test, rectangular shape samples with the size of 2x3x20 mm^3 were cut by the electric discharge. Three points bending tests were performed using a Shimadzu AGS-J test machine with the crosshead speed of 0.5mm/min and the span of 15mm.

3 EXPERIMENTAL RESULTS AND DISCUSSION

Figure 1 shows the X-ray diffraction pattern from the cross section of the sintered TiB_2-AlFe composite specimens of 85 wt% TiB_2 sintered at 1373K, 85wt%TiB_2 sintered at 1573K and 90wt%TiB_2 sintered at 1373K. In Fig. 1, diffraction peaks from cubic AlFe and hexagonal TiB_2 have been observed in all three diffraction patterns showing that AlFe and TiB_2 consists of pseudo-binary eutectic phase diagram as proposed by K. Matsuura et al.[5] The ratio of the intensity of the diffraction peaks from AlFe to those from TiB_2 decreases as sintering temperature increases from 1373K to 1573K. The diffraction intensity from AlFe of the 85wt% TiB_2 specimen sintered at 1573K is nearly the same as that of the 90wt%TiB_2 specimen sintered at 1373K suggesting that one third of AlFe in the former specimen disappeared during sintering at 1573K. It seems that evaporation of AlFe becomes significant at 1573K. Hereafter we refer the specimens by the starting powder compositions.

Figure 2 (a), (b) and (c) show the SEM images of the cross-section of the TiB_2-AlFe composite specimens with 85wt%TiB_2 sintered at 1373K, 1473K and 1573K, respectively. In Fig. 2 (a) no pore is observed and dense specimen is obtained. The diameter of TiB_2 grains is around 0.2 μm when sintered at 1373k which is far smaller than those obtained by the combustion synthesis method. [4-6] As the sintering temperature increases to 1473K, coarsening of the TiB_2 grains proceeds and the grain size becomes around 0.5 to 1.0 μm. The grain size increases to several microns as the sintering temperature increases to 1573K as shown in Fig. 2 (c).

The bending strength of the TiB_2-AlFe composite specimens with 85wt%TiB_2 and 90wt%TiB_2 sintered at 1373K and 1573K are summarized in Table 1. The bending strength as high as 850MPa has been obtained for the specimen with 85wt% TiB_2 sintered at 1373K. The bending strength decreases as the sintering temperature increases to 1573K. This decrease of the bending strength may be caused by the decrease of the amount of AlFe as the sintering temperature increases to 1573K because it is supposed that the bonding strength between TiB_2 grains are weaker than that between AlFe and TiB_2 grains. The bending strength of the specimen with 90wt%TiB_2 is smaller than that of the specimen with 85wt% TiB_2.

The Vickers hardness of the TiB_2-AlFe composite specimens with 85wt%TiB_2 and 90wt%TiB_2 are summarized in Table 2. The Vickers hardness as high as around 2300 Hv and 2400 Hv has been obtained for the specimens with starting composition of 85wt% and 90wt%, respectively.

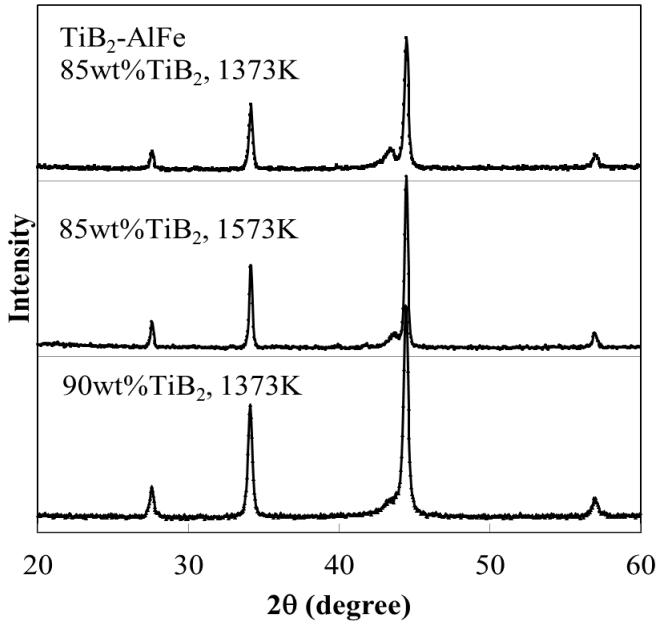

Figure 1: X-ray diffraction pattern from the cross section of the TiB_2-AlFe composite specimens of 85 wt% TiB_2 sintered at 1373K, 85wt%TiB_2 sintered at 1573K and 90wt%TiB_2 sintered at 1373K.

Figure 3 shows the SEM image of the Vickers indentation of the TiB_2-AlFe composite specimen with 85wt%TiB_2 sintered at 1373K (a) or 1573K(b) indented with the load of 19.6N. In Fig. 3 (a) it has been shown that no tipping occurs and clear pyramid shape is indented. Vickers hardness is estimated as 2320 ± 40Hv from the area of the indentation. On the other hand, in Fig. 3 (b), tipping occurs and the shape becomes distorted. This may be caused by the non-uniform mechanical properties of the specimen due to large grain growth of TiB_2 and/or AlFe.

Figure 4 shows the enlarged image of the Vickers indentation of the area encircled in Fig. 3 (a). It has been observed that a crack emanates from a corner of the indentation. The crack runs not straight but is winding along the interface between TiB_2 and AlFe matrix. Cracks are observed along the edge of indentation, also.

In Fig. 5 is shown the SEM images of the Vickers indentation indented with the load of 98N and 490N. No chipping has been observed even if the load is increased to 490N. In table 3 is summarized the crack length of the indentation in the TiB_2-AlFe composite specimen with 85wt%TiB_2 sintered at 1373K for the load between from 19.6N to 490N.

Various models to deal with indentation fracture have been proposed which are reviewed by Ponton and Rawlings. [9] The indentation fracture models reported in the literature are classified into two groups, in one group it is assumed that the cracks which form as a result of Vickers indentation are well developed radial-median halfpenny-shaped cracks, and in the other group it is assumed that radial Palmqvist cracks are formed. These two types of cracks are shown schematically in Fig. 6.

For the radial-median halfpenny shaped cracks, the following equation is proposed to obtain the critical stress intensity factor for indentation fracture, K_c, as

$$K_c = 0.0824P/c^{3/2} \quad (1),$$

where P is the indentation load, and c is the crack length measured from the indentation centre (see Fig. 6). For the Palmqvist type cracks, the following equation is proposed as,

$$K_c = 0.0329P/al^{1/2} \quad (2),$$

where *P* is the indentation load, *a* half length of the indentation diagonal and *l* the crack length.

The empirical criterion for the halfpenny cracks is the ratio *c/a* larger than 2. In the present experiment, this criterion has been satisfied for the cracks generated with the load value of 294N and 490N. The K_c obtained from eq. (1) is 13MPa·$m^{1/2}$. On the other hand, cracks generated with the load of 19.6N seems to be the Palmqvist type. The K_c value is 12 MPa·$m^{1/2}$ obtained from the crack generated by the load value of 19.6N using eq. (2).

Li et al fabricated AlFe-80vol%TiB_2 composite by the combustion synthesis method and measured the Vickers hardness and fracture toughness [6]. Their value is 1800Hv and 6MPa·$m^{1/2}$. Both of the Vickers hardness and the fracture toughness of AlTi-TiB_2 composite with sub-micron sized TiB_2 grains is superior than those of FeAl-TiB_2 composite with micron sized grains.

WC-Co composite materials have been investigated intensely and commercialized as cutting tools. Laugier performed the Vickers test of WC-Co composites of various composition and investigated the indentation crack length. [10] They have shown that the Vickers hardness increases while the crack length increases (K_c value decreases) as the amount of WC increases. The hardest specimen shown in ref. 10 noted as '3F' has Vickers hardness of around 2000Hv. The crack length, *l*, of the '3F' specimen is 150μm (250 μm) for the indentation load of 294N (490N). The Vickers hardness and K_c value of the AlFe-85wt%TiB_2 specimen are larger than those of the WC-Co '3F' composite.

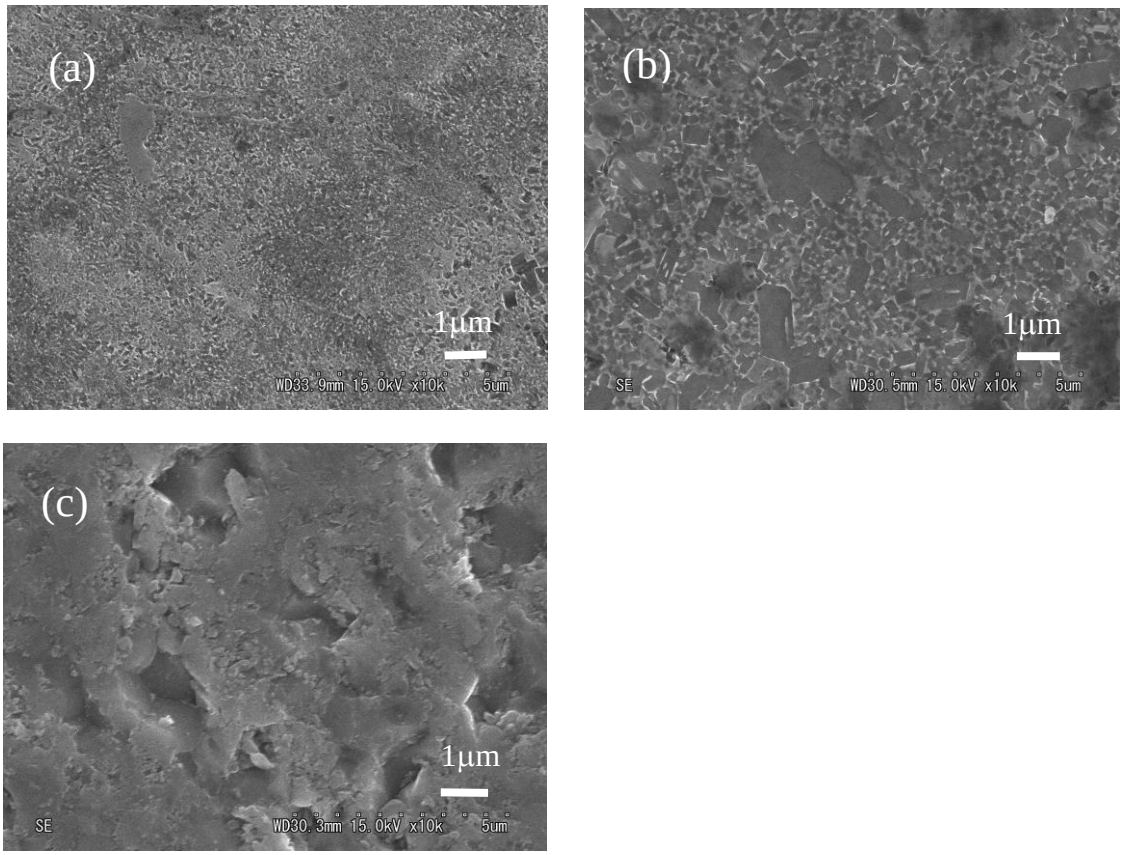

Figure 2: SEM images of the TiB_2-AlFe with 85wt%TiB_2 sintered at 1373K (a), 1473K (b) and 1573K (c).

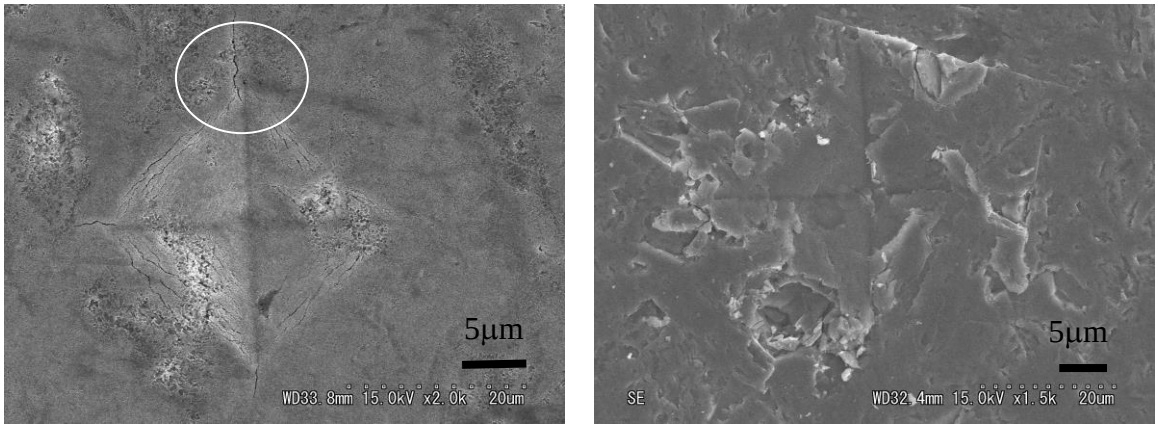

Figure 3: SEM images of the Vickers indentation in TiB_2-AlFe composite specimens with 85wt%TiB_2 sintered at 1373K (a) and 1573K (b) indented with the load of 19.6N.

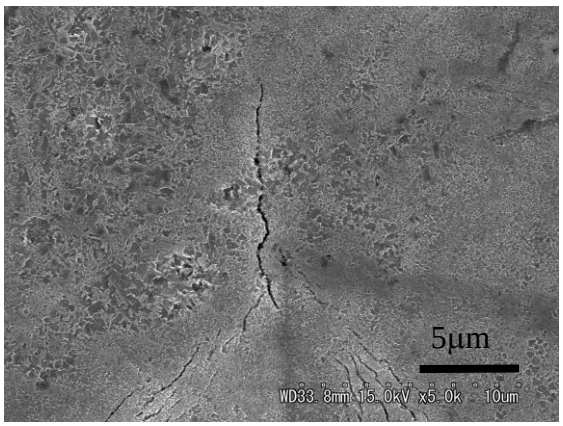

Figure 4: Enlarged image of the encircled area in Fig. 3 (a)

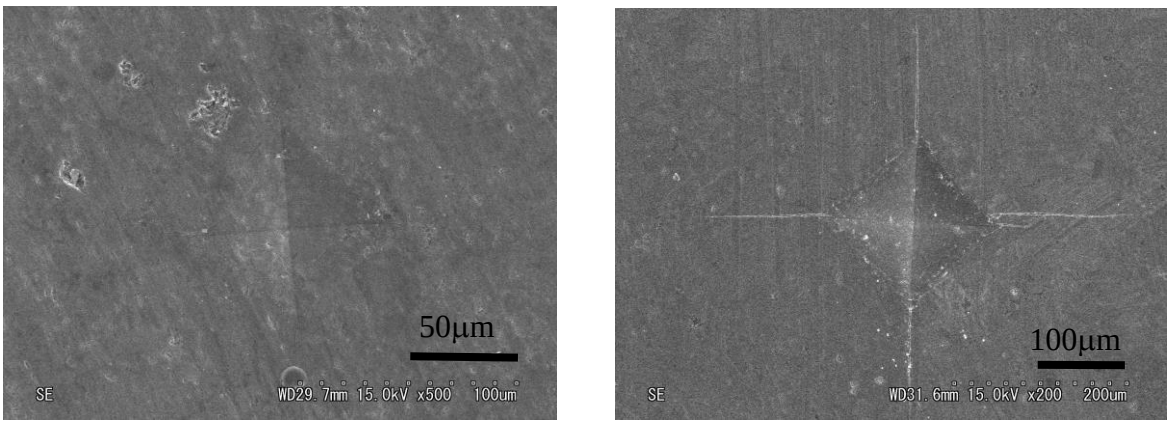

Figure 5: SEM images of the Vickers indentation of the TiB_2-AlFe composite specimen with 85wt%TiB_2 sintered at 1373K indented with the load of (a) 98N and (b) 490N.

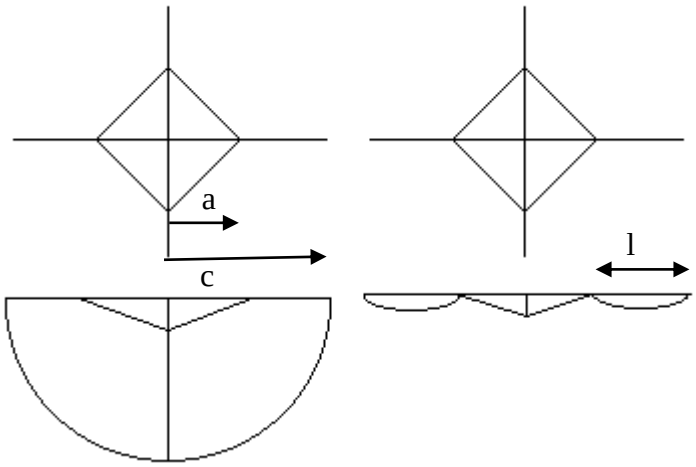

Figure 6: Schematic plan view and cross-sectional view of a Vickers indent radial-median halfpenny crack system (a) and radial Palmqvist crack system (b).

	85wt%, 1373K	85wt%, 1573K	90wt%, 1373K	90wt%, 1573K
Bending Strength	850MPa	620MPa	670MPa	520MPa

Table 1: The bending strength of the TiB_2-AlFe composite specimens.

	85wt%, 1373K	85wt%, 1573K	90wt%, 1373K	90wt%, 1573K
Bending Strength	2320±40 Hv	2340±40 Hv	2400±60 Hv	2450±60 Hv

Table 2: The Vickers hardness of the TiB_2-AlFe composite specimens.

	a(μm)	*c*(μm)	*l*(μm)	Hv	K_c (MPa·$m^{1/2}$)
2kg	20	27	7	2320	12*
10kg	44	69	25	2390	14**
30kg	76	155	79	2410	13**
50kg	100	218	118	2320	13**

Table 3: Indentation parameters and toughness values obtained for the TiB_2-AlFe composite specimen with 85wt%TiB_2 sintered at 1100C. The definitions of *a*, *c*, and *l* are shown in Fig. 6. K_c values indicated by *are obtained using eq. (1) and ** using eq. (2).

4 CONCLUSIONS

We have fabricated TiB_2-AlFe composite by the reaction sintering of Ti , B, Al and Fe powders using spark plasma sintering. We have succeeded to obtain dense TiB_2-AlFe specimens up to 85wt% (88vol%) of TiB_2 by the sintering at 1373k. It is shown that TiB_2 particles is dispersed uniformly in the FeAl matrix. The size of TiB_2 particles is around 0.2 μm when sintered at 1373K, which increases to 0.5 μm at 1473K. The Vickers hardness as high as 232 0Hv and bending strength of 850MPa has been obtained. The fracture toughness estimated from the indentation crack is 13MPa·$m^{1/2}$. It has been shown that TiB_2–AlFe composite has high hardness, high strength and excellent fracture toughness.

ACKNOWLEDGEMENTS

This work is supported by the Grant-in-Aid for Science Research from Japan Society for the promotion of Science (Kakenhi 16K06803)

REFERENCES

[1] G.V. Samsonov and I.M. Vinitskii, *Handbook of Refractory Compounds*, IFI/Plenum, New York, 1980.

[2] W. Wang, Z. Fu, H. Wang and R. Yuan, Influence of hot pressing sintering temperature and time on microstructure and mechanical properties of TiB_2 ceramics, *J. European Ceramics Society*, 22, 2002, pp. 1045-1049.

[3] R.D. Torres, I.E. Reimans, J.J. Moore and G.G.W. Mustoe, Reaction steps in the combustion synthesis of NiAl/TiB_2 composites, *Metallurgical and Materials Transactions B*, 31B, 2000, pp. 433-438.

[4] K. Matsuura, Y. Obara and M. Kudoh, Fabrication of TiB_2 particle dispersed FeAl-based composites by self-propagating high-temperature synthesis, ISIJ International, 46, 2006, pp. 871-874.

[5] K. Matsuura, Y. Obara and K. Kojoma, Combustion synthesis of boride particle dispersed hard metal from elemental powders, *Int. Journal of Refractory Metals & hard materials*, 27, 2009, pp. 376-381.

[6] Y. Li, K. Matsuura, M. Ohno, Y.M. Gao and J. Yu, Combustion synthesis of TiB_2 based hard material cemented by Fe-Al intermetallics, *Powder Metallurgy*, 55, 2012, pp. 162-167.

[7] M. Yoshida, Influence of sintering temperature on the microstructure of TiB_2 sintered with Al_3Ti Additive, *Materials Transaction*, 53, 2012, pp. 1648-1652.

[8] M. Yoshida and T. Yumitate, Mechanical properties of TiB_2-Al_3Ti and TiB_2-$(Al,Ni)_3Ti$ composites, *Materials Transaction*, 53, 2012, pp.1933-1937.

[9] C.B. Ponton and R.D. Rawlings, Vickers indentation fracture toughness test part 1 review of literature and formulation of standardized indentation toughness equations, *Material Science and Technologies*, 5, 1989, pp. 865-872.

[10] M.T. Laugier, Palmqvist indentation toughness in WC-Co composites, *J. Material Science Letters*, 6, 1987, pp. 897-900.